Rare Metal Materials and Engineering
Volume 47, Issue 11, November 2018
Online English edition of the Chinese language journal

Available online at www.sciencedirect.com

ScienceDirect

Cite this article as: Rare Metal Materials and Engineering, 2018, 47(11): 3272-3276.

ARTICLE

Transmission Electron Microscopic Observation of a Novel Al_3Zr-η' Core-shell Particle in Al-Zn-Mg-Cu Alloy

Liu Fei, Bai Pucun, Hou Xiaohu, Tong Naiqiang, Cui Xiaoming

Inner Mongolia University of Technology, Hohhot 010051, China

Abstract: The Al_3Zr-η' core-shell particles were observed in the Al-12Zn-2.4Mg-1.1Cu-0.5Ni-0.2Zr alloy using high-resolution transmission electron microscopy (HRTEM) and selected area electron diffraction (SAED). Two types of Al_3Zr particles appear in the Al matrix: one is a standalone Al_3Zr particle that is coherent with the matrix, and the other is an as-core Al_3Zr particle actingas a nucleation site of the η' precipitates, resulting in a core-shell particle which is semi-coherent with the matrix. The shell is composed of η' precipitates with four variants. The strain in the as-core Al_3Zr is lower than that in the standalone Al_3Zr, and a considerable amount of strain exists across the interfacial regions between the η' precipitates and the matrix.

Key words: aluminum alloy; heterogeneous nucleation; HRTEM;SAED ; geometric phase analysis

As precipitation hardened aluminum alloys, Al-Zn-Mg-Cu series are extensively used as structural components due to the formation of a fine coherent GP zone and semi-coherent η' precipitates, causing a significant improvement in mechanical properties[1,2]. It has been reported that the peak hardening of Al-Zn-Mg-Cu alloys is dominated by the fine distribution of η' precipitates[3, 4]. Many researchers studied the nucleation of η' precipitates in supersaturated Al matrix and reported that η' heterogeneously precipitates on sites such as GP zones[5, 6], grain boundaries[7-10], dislocation lines[11, 12], and interfaces between second phases and the matrix[13]. It is said that the reduction of interface energy or the increment of nuclear driving force causes such phase transformation[7, 9]. The coherent Al_3Zr (Al_3Sc, Al_3Li) dispersion with an $L1_2$ structure is a second phase material, which is generally used to inhibit the recrystallization and restrain grain growth in commercial aluminum alloys[10, 14-17]. In particular, they can also act as nucleation cores in other Al alloys. For instance, Al_3Zr-δ' core-shell particles were observed in Al-Li-Zr alloys, Al_3Zr-θ'core-shell particles were observed in Al-Li-Cu-Zr alloys[18], Al_3Sc-Al_3Zr core-shell particles were observed in Al-Sc-Zr alloys[14, 19], and Al_3(LiScZr) core-shell particles were observed in Al-Li-Sc-Zr alloys[20]. However, the formation of Al_3Zr-η' core-shell particles in Al-Zn-Mg-Cu alloys is seldom reported elsewhere.

In this study, an Al_3Zr-η' core-shell particle was observed in -Zn-Mg-Cu alloy using high-resolution transmission electron microscopy (HRTEM). Combining selected area electron diffraction (SAED) simulation with geometric phase analysis (GPA), the structure of the particles and the interfacial lattice distortions between the Al_3Zr-η' core-shell particle and the Al matrix were investigated.

1 Experiment

The experimental sample was synthesized via a spray forming technique with the nominal composition (wt%) of 12 Zn, 2.4 Mg, 1.1 Cu, 0.5 Ni, 0.2 Zr, and balance Al [21]. The solution treatment was conducted at 758 K for 2 h, followed by water-quenching to room temperature (298 K). Finally, the artificial aging of the alloy was conducted at 393 K for 8 h. For the microstructure analysis, the TEM specimens were first prepared by mechanical polishing followed by twin jet electropolishing. A JEM-2010 transmission electron microscope operated at 200 kV was used to perform HRTEM

Received date: November 25, 2017
Foundation item: National Natural Science Foundation of China (11362014, 11672140); Specialized Research Fund for the Doctoral Program of Higher Education of China (20131514110004)
Corresponding author: Bai Pucun, Ph. D., Professor, College of Materials Science and Engineering, Inner Mongolia University of Technology, Hohhot 010051, P. R. China, Tel: 0086-471-6575790, E-mail: pcbai@163.com

investigations. The electron beam along the $[110]_{Al}$ direction was used to obtain the micrographs. Lattice distortion was analyzed using GPA software built-in with the Gatan Digital Micrograph software. Furthermore, the Al matrix remote from the particles was used for reference to the undistorted lattice. Masks were set around the $(1\bar{1}\bar{1})$ and $(\bar{1}1\bar{1})$ reflections of the Al matrix.

2 Results and Discussion

2.1 Microstructures

Fig.1 shows the selected area electron diffraction (SAED) patterns of the experimental alloy after aging for 8 h at 393 K. The strong diffraction spots originate from the Al matrix, and the spots at $\{001\}_{Al}$ and $\{110\}_{Al}$ from the $L1_2$-Al_3Zr dispersion are observed (Fig.1a and 1b). Some weak diffraction spots located at 1/3 and 2/3 of {220} Al matrix reflection are also observed. In addition, streaks from $(1\bar{1}\bar{1})$ and $(\bar{1}1\bar{1})$ reflections are found in the pattern (Fig. 1a). Compared with the diffraction characteristics of precipitates in other Al-Zn-Mg-Cu alloys[3, 4], it can be concluded that the η' phase is the major precipitate.

Dark field micrograph of the experimental alloy in Fig.2a

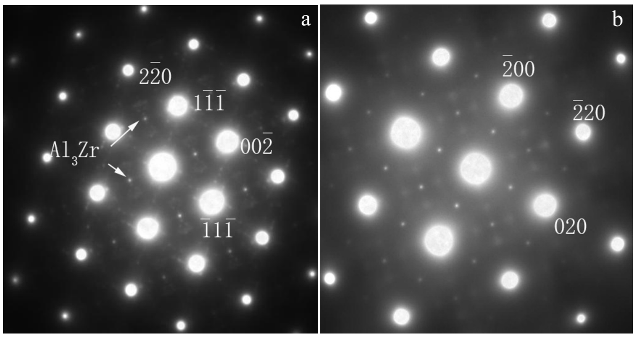

Fig.1 Selected area electron diffraction patterns of the experimental alloy taken along $[110]_{Al}$ (a) and $[100]_{Al}$ (b) zone axis

are obtained by selecting [001] superlattice reflection, where the distribution of Al_3Zr dispersoids is shown. Al_3Zr particles with a size of ~20 nm in the Al matrix can be seen. The nature of the Al_3Zr dispersoid was also studied using TEM under two beam conditions, as shown in Fig.2b and 2c. Some of the Al_3Zr particles display a contrast of "coffee bean", as shown by the yellow arrows in Fig.2b and 2c. However,other Al_3Zr particles present a "dark dot" contrast (Fig.2b) or a "bright dot" (Fig.2c) contrast instead of "coffee bean", as shown by the red triangles in the images.

Fig.3a shows a HRTEM image of Al_3Zr particles with a "coffee bean" as acontrast . The "coffee bean" contrasted Al_3Zr particles is standalone Al_3Zr particle in the Al matrix, which is consistent with previously published studies[10, 15, 16, 22-25]. It is thought that the "coffee bean" contrast is a strain contrast caused by the lattice parameter misfit of the spherically symmetrical coherent inclusion[26]. It is interesting that the Al_3Zr particle with a "bright dot" or "dark dot" contrast presents a core-shell structure, as shown in Fig.3b. The core has a diameter of 3.5 nm, and the shell has a thickness of 2.9 nm, which is shown by blue and yellow dashed lines, respectively (Fig.3b).

To investigate the structure of the core-shell Al_3Zr particles, the HRTEM image and the corresponding inverse Fourier transform were first employed. The HRTEM image of the core-shell Al_3Zr particle (magnified box region in Fig.2c) and the corresponding inverse Fourier transform using the vector $\boldsymbol{g}_{001}$ are shown in Fig.4a and 4b, respectively. It is clear that the Al_3Zr particle serves as a core in the core-shell composite particle. However, part of the standalone Al_3Zr particle is also observed at the top left corner of Fig.4a, as depicted by the blue line. The Fourier transform of the HRTEM image is displayed in the bottom -left, as shown in the inset of Fig.4b. The extra diffraction spots (see the inset of Fig.4b) are consistent with the SAED pattern shown in Fig.1a. Therefore, it is reasonable to speculate that η' precipitations can act as a shell in the core-shell composite particles.

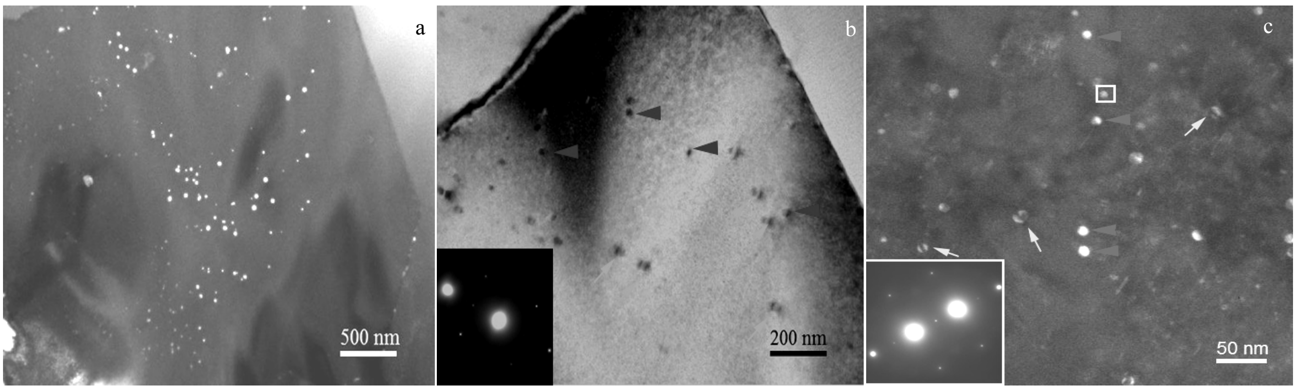

Fig.2 Dark field micrograph obtained by $(00\bar{1})$ superlattice reflection (a), two-beam condition bright field micrograph viewed with $\boldsymbol{g}(\bar{2}20)$ of the sample near $[100]_{Al}$ (b), and two-beam condition dark field micrograph viewed with $\boldsymbol{g}(0\bar{2}0)$ of the sample near $[100]_{Al}$ (c)

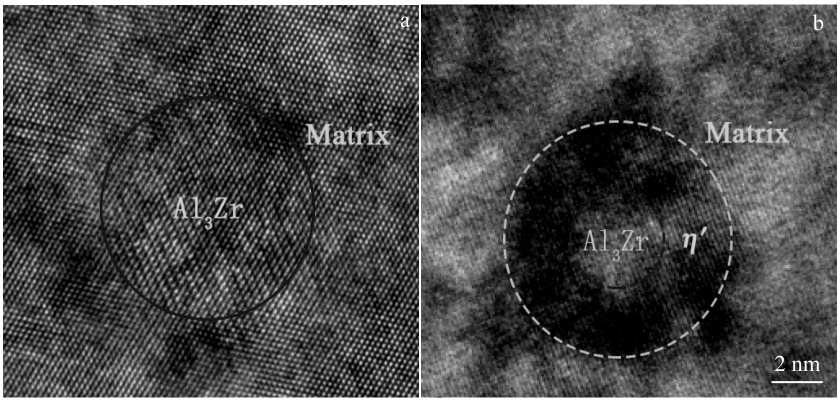

Fig.3 HRTEM images of standalone Al_3Zr (a) and Al_3Zr (b) particle with core-shell structure

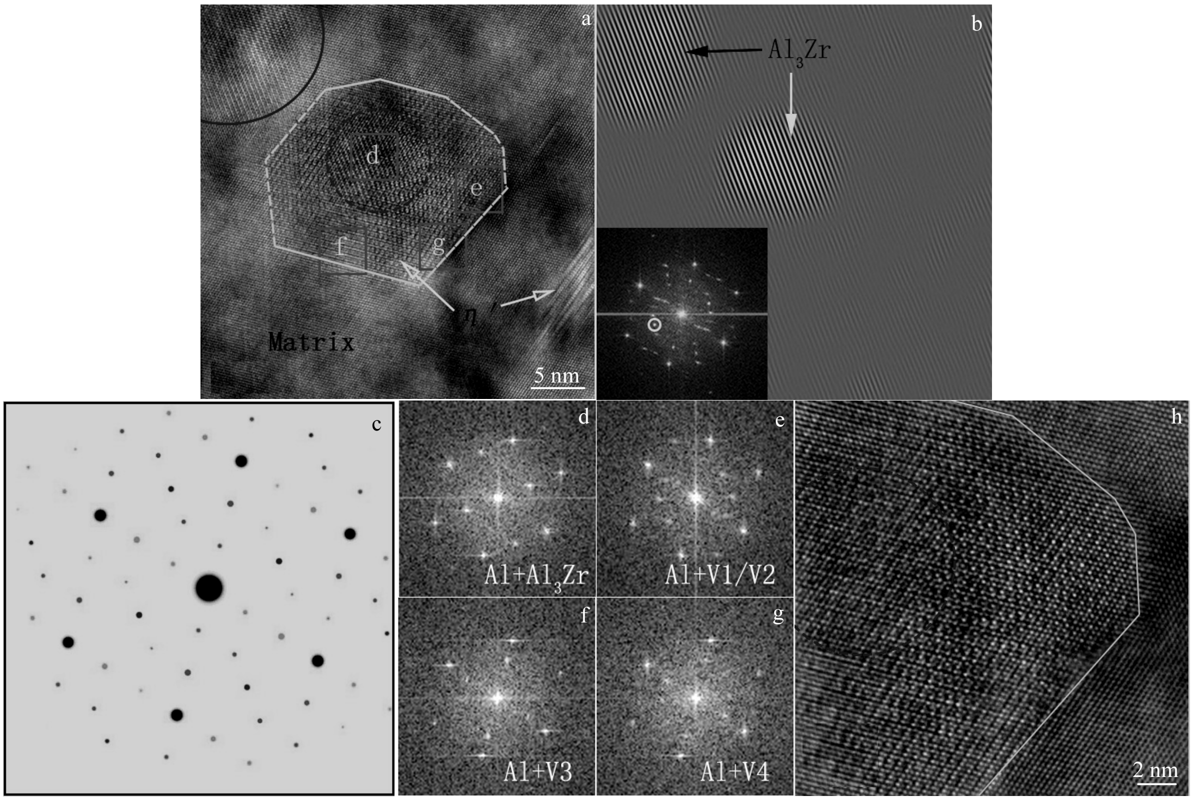

Fig.4 HRTEM image showing a core-shell particle in the Al matrix (a); inverse Fourier transform image using vector $\boldsymbol{g}_{001}$, showing an Al_3Zr-core, as indicated by white arrows (b); the simulated patterns including four variants of the η' phase, the Al matrix, as well as the Al_3Zr dispersoid along the $[110]_{Al}$ zone axes (c), diffraction spots from Al_3Zr, variant 1 (or variant 2), variant 3, variant 4, and the Al matrix are indicated with blue, red, green, bright green, and black, respectively; Fourier transform images taken from corresponding zones in Fig.4a (d~g); magnified core-shell particle corresponding to Fig.4a (h)

Secondly, electron diffraction simulations were used to verify the speculation. As the main contributor of aging of Al-Zn-Mg-Cu alloys, special attention has been paid on η' precipitate hardening[3, 4, 27, 28]. Although the composition of it is still unclear, the crystal structure of the η' precipitate has been widely suggested to have a hexagonal structure with lattice parameters a = 0.496 nm and c =1.402 nm[1-4]. There is a well-defined orientation relationship, $(10\bar{1}0)_{\eta'}//\{110\}_{Al}$, $(0001)_{\eta'}//(111)_{Al}$, $(\bar{1}\bar{1}20)_{\eta'}//(112)_{Al}$, between the η' precipitate and the Al matrix. In this study, Kverneland's model (II)[28] with $Mg_2Zn_{5-x}Al_{2+x}$ (x=2~4) composition and a space group P63/mmc are used to simulate diffraction patterns. Considering the four equivalents (111) in fcc, the orientation relationship between η' precipitate and Al matrix can be classified into four variants, named variant 1, variant 2, variant 3, and variant 4[4, 28]. Fig. 4c shows the simulated diffraction patterns that include four variants of the η' phase, the Al matrix, and the Al_3Zr dispersoid taken along the $[110]_{Al}$ zone axes. It is important to note that, although variants 1 and 2 havedifferent orientations, their diffraction spots are located at the same position along $[110]_{Al}$.

Then, Fourier transform images taken from corresponding zones in Fig. 4a are shown in Fig. 4d~4g. Compared to the characteristics of the images, the experimental results are consistent with the simulated diffraction patterns. The four objects shown in Fig. 4d, 4e, 4f, and 4g can be denoted as Al_3Zr, variant 1 (V1) or variant 2 (V2), variant 3 (V3), and variant 4 (V4), respectively. No obvious interface is visible among the variants (Fig. 4h). This can be due to the symmetry of interfaces on the projected image or the coherency between variants in a certain orientation. Based on the above results, it was be verified that the η' precipitate act as a shell in the core-shell composite particle.

2.2 Strain field

Taking the x-axis parallel to $[1\bar{1}\bar{1}]_{Al}$, the plane strain component ε_{xx} calculated by GPA is shown in Fig. 5a. Some convergence regions of strain near the interface between η' precipitates and the matrix, or between η' precipitates and Al_3Zr, reveal that some dislocations exist as a result of the the semi-coherent interface. The intermediate region between the convergence regions presents considerable strains along the interface (appearing in blue or red color) such as region 1 and 2 shown in Fig. 5a Fig. 5b shows the strain profile measured across the interface in Region 1 along the length of the box shown by Line 1 in Fig. 5a. The strain profile was averaged over the width of Line 1. Strain saltation (about −5.5%) was measured across this region, revealing the compressive strain of Al matrix and the tensile strain of η' precipitates. Similarly, another strain profile from Line 2 shown in Fig. 5b reveals the tensile strain (about +2.7%) of the Al matrix and the compressive strain of the η' precipitates. Fundamentally, the strain difference between Line 1 and 2 results from different orientations in the interface. These results are close to those reported by Wolverton[27], the η' precipitates in the 7000 series Al alloys are under large strain: 5.7% tensile strain along $[0001]_{\eta'}$ and 3.4% compressive strain along $[1010]_{\eta'}$.

Moreover, it should be noted that there are slight differences of strain component ε_{xx} in color between the standalone Al_3Zr (depicted by the blue line in the top-left corner in Fig. 3a) and the as-core Al_3Zr particle. The statistical mean strain value of the standalone Al_3Zr particle is 0.00341297. This agrees well with the theoretical lattice misfit δ= 0.004 099 78, calculated by selecting a lattice parameter of 0.4049 nm in single phase Al (JCPDS file No. 89-4037) and 0.406 56 nm in $L1_2$-Al_3Zr[29]. The statistical mean strain value of the as-core Al_3Zr particle of −0.001 630 1 is lower than that of the standalone particle.

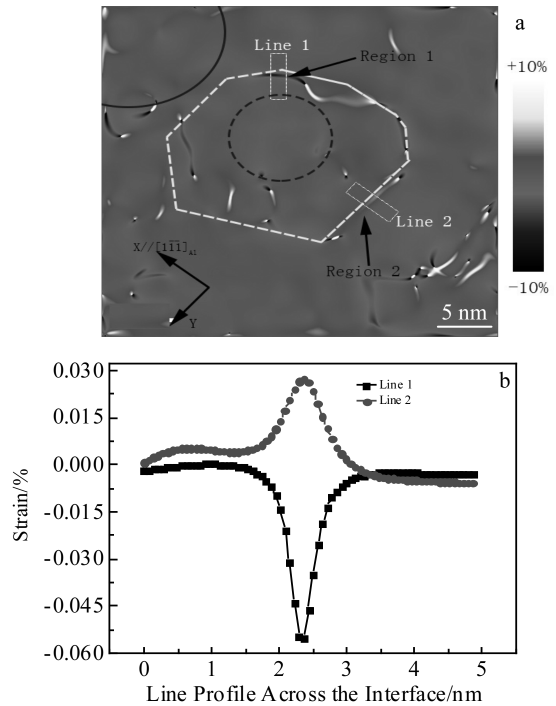

Fig. 5 Strain components ε_{xx} obtained from Fig. 2a via the geometric phase analysis technique (a), and strain profiles measured across the interface along the length and averaged over the width of the box shown as Line 1 and Line 2 in Fig. 5a (b)

Usually, core-shell precipitates in alloys display cores and shells made of two phases with similar structures[16, 18]. Interestingly, the core here is a cubic phase, while the shell is formed by a phase with a hexagonal structure. A possible mechanism can be speculated that the interfacial lattice distortion is beneficial to the nucleation of η' precipitates on the $L1_2$-Al_3Zr particle. Further work confirming the mechanism is required. In addition, due to the semi-coherent relation between η' precipitates and the matrix, or between η' precipitates and $L1_2$-Al_3Zr, the Al_3Zr-η' core-shell particles have no strain contrast in the two-beam bright field TEM, as shown in Fig. 2b. This phenomenon is similar to that in Ref.[22], where the strain contrast disappeared in the Al-Zn-Mg alloys when the $Al_3(Sc,Zr)$ dispersoid loses coherency.

3 Conclusions

1) Two types of Al_3Zr particles appear in the Al matrix: one is a standalone Al_3Zr particle coherent with the matrix, and the other is an as-core Al_3Zr particle, which acts as a nucleation core for η' precipitates, resulting in a core-shell structure particle which is semi-coherent with the matrix.

2) The mean strain of the as-core Al_3Zr is −0.16%, which is lower than 0.34% of the standalone mean strain. The shell is composed of η' precipitates with four variants. Strains caused

by the misfit dislocation are mainly generated at the interface of matrix/η' phase. The maximum strain along $[1\bar{1}\bar{1}]_{Al}$ is 5.5%.

References

1 Chen Gang, Chen Wei, Zhang Guowei *et al. Rare Metal Materials and Engineering*[J], 2016, 45(9): 2237

2 Xu Yongqian, Zhan Lihua, Li Shujian *et al. Rare Metal Materials and Engineering*[J], 2017, 46(2): 355

3 Yu H C, Wang M P, Jia Y L *et al*. *Journal of Alloys and Compounds*[J], 2014, 601: 120

4 Yang W C, Ji S X, Wang M P *et al*. *Journal of Alloys and Compounds*[J], 2014, 610: 623

5 Sha G, Cerezo A. *Acta Materialia*[J], 2004, 52(15): 4503

6 Berg L K, Gjonnes J, Hansen V *et al. Acta Materialia*[J], 2001, 49(17): 3443

7 Lin Y C, Xia Y C, Jiang Y Q *et al. Materials Science and Engineering A*[J], 2012, 556: 796

8 Tiryakioğlu M, Robinson J S, Eason P D. *Materials Science and Engineering A*[J], 2014, 618: 22

9 Lang Y J, Cai Y H, Cui H *et al. Materials & Design*[J], 2011, 32(8-9): 4241

10 Liu Jing, Yao Pei, Zhao Naiqin *et al. Journal of Alloys and Compounds*[J], 2016, 657: 717

11 Fribourg G, Bréchet Y, Chemin J L *et al. Metallurgical and Materials Transactions A*[J], 2011, 42(13): 3934

12 Lin Y C, Zhang Jinlong, Chen Mingsong. *Journal of Alloys and Compounds*[J], 2016, 684: 177

13 Deschamps A, Bréchet Y. *Materials Science and Engineering A*[J], 1998, 251(1-2): 200

14 Tolley A, Radmilovic V, Dahmen U. *Scripta Materialia*[J], 2005, 52(7): 621

15 Jia Z H, Couzinie J P, Cherdoudi N *et al*. *Transactions of Nonferrous Metals Society of China*[J], 2012, 22(8): 1860

16 Jia Zhihong, Hu Guiqing, Forbord Børge *et al. Materials Science and Engineering A*[J], 2007, 444(1-2): 284

17 Zhang Wei, Xing Yuan, Jia Zhihong *et al. Transactions of Nonferrous Metals Society of China*[J], 2014, 24(12): 3866

18 Kanno Motohiro, Ou Binlung. *Materials Transactions, JIM*[J], 1991, 32: 445

19 Radmilovic V, Ophus C, Marquis E A *et al. Nature Materials*[J], 2011, 10(9): 710

20 Radmilovic V, Tolley A, Marquis E A *et al. Scripta Materialia*[J], 2008, 58(7): 529

21 Bai P C, Hou X H, Zhang X Y *et al. Materials Science and Engineering A*[J], 2009, 508(1-2): 23

22 Schobel M, Pongratz P, Degischer H P. *Acta Materialia*[J], 2012, 60(10): 4247

23 Fang H C, Chen K H, Chen X *et al. Corrosion Science*[J], 2009, 51(12): 2872

24 Wu H, Wen S P, Huang H *et al. Journal of Alloys and Compounds*[J], 2016, 685: 869

25 Xiao Tao, Deng Yunlai, Ye Lingying *et al. Materials Science and Engineering A*[J], 2016, 675: 280

26 Ashby M F, Brown L M. *Philosophical Magazine*[J], 1963, 8(91): 1083

27 Wolverton C. *Acta Materialia*[J], 2001, 49(16): 3129

28 Kverneland A, Hansen V, Vincent R *et al*. *Ultramicroscopy*[J], 2006, 106(6): 492

29 Guo J Q, Ohtera K. *Materials Letters*[J], 1996, 27(6): 343

Al-Zn-Mg-Cu 合金中一种新型 Al_3Zr-η'核壳颗粒的透射电子显微镜观察

刘 飞，白朴存，侯小虎，佟乃强，崔晓明

(内蒙古工业大学，内蒙古 呼和浩特 010051)

摘　要：利用高分辨透射电子显微镜(HRTEM)和选区电子衍射(SAED)观察了 Al-12Zn-2.4Mg-1.1Cu-0.5Ni-0.2Zr 合金中的 Al_3Zr-η'核壳颗粒。结果发现：Al_3Zr 颗粒在合金基体中以 2 种形态存在，一种是与基体共格单独存在的 Al_3Zr 颗粒；另外一种是作为 η'析出相形核位置的核心 Al_3Zr 颗粒，形成了一种与基体半共格的 Al_3Zr-η'核壳颗粒。该核壳颗粒的壳层由 4 种 η'析出相变体组成。核心 Al_3Zr 颗粒内部的晶格变形低于单独存在的 Al_3Zr 颗粒，η'析出相和基体界面处存在显著的晶格应变。

关键词：铝合金；异质形核； HRTEM；SAED；几何相位分析

作者简介：刘 飞，男，1986 年生，博士生，内蒙古工业大学材料科学与工程学院，内蒙古 呼和浩特 010051，电话：0471-6577161，E-mail: ngdliufei@163.com